Novel Preparation and Properties of EPDM/Montmorillonite Nanocomposites

BaoLei Liu,[1] QingJun Ding,[1] QiHui He,[1] Jun Cai,[1] BaiXing Hu,[1] Jian Shen[1,2]

[1]College of Chemistry and Chemical Engineering, Nanjing University, Nanjing 210093, People's Republic of China
[2]College of Chemistry and Environment Science, Nanjing Normal University, Nanjing 210097, People's Republic of China

ABSTRACT: This article reports on a novel route to develop ethylene–propylene–diene rubber (EPDM)/montmorillonite nanocomposites Modification of the MMT was carried out with maleic anhydride (MA), which acts as the intercalation agent for MMT and the vulcanizing agent for EPDM matrix, as well as the compatibilizer for the EPDM and MMT phases. The effect of MA-modified MMT in nanocomposites was investigated by focusing on three major aspects: structural analysis, thermal properties, and material properties. The d-spacings of both the MA modified MMT and exfoliated nanocomposites were investigated by X-ray diffraction (XRD), and the morphology of these nanocomposites was examined by transmission electron microscopy (TEM) and scanning electron microscopy (SEM). Dynamic mechanical analysis confirms the constraint effect of exfoliated MMT layers on EPDM chains, which benefited the increased storage modulus, increased glass transition temperature. Thermogravimetric analysis indicates that there is some enhancement in degradation behavior between the nanocomposites and EPDM matrix. The nanocomposites exhibit great improvement in tensile strength and modulus, as well as elongation-at-break. The effects of MA addition on the formation of nano-metric reinforcement and on the mechanical properties of nanocomposites are discussed. © 2005 Wiley Periodicals, Inc. J Appl Polym Sci 99: 2578–2585, 2006

Key words: EPDM; clay; melt; nanocomposites; exfoliation

INTRODUCTION

Nanocomposite materials contain inorganic phase at the nanometer scale. Since a montmorillonite (MMT)-reinforced Nylon nanocomposite was developed by Toyota in 1987,[1] polymer/layered silicate nanocomposites have been receiving significant research attention, because they often exhibit remarkable improvement of mechanical, thermal, optical, and physio-chemical properties when compared with the pure polymer or conventional composites.[2–6] These improvements include increased strength and storage modulus, heat and solvent resistance, and more efficient gas barrier with low inorganic loadings, because of the nanometer-size dispersed particles.

To achieve a nano-scale dispersion of silicates in a polymer matrix, the silicates are generally pretreated with alkylammonium ions to produce an organoclay.[7] This treatment is effective in opening up the gallery of silicate, and the organo-clays can then be easily dispersed in the polymer matrix and form nanocomposites with an intercalated or exfoliated structure. In the former case, the spacing between the silicate layers is increased by the incorporation of extended polymer chains into the layers. In exfoliated nanocomposites, unstacked organo-clay blocks are dispersed individually throughout the polymer matrix.[8] Though alkylammonium ions are easy to open up the gallery of silicate, they may not introduce high interfacial interactions between the polymer matrix and silicate. So, the introduction of polar groups such as –COOH along the gallery of silicate, which can increase the potential binding energy,[9] becomes necessary. Maleic anhydride (MA) can easily enter the galleries of acid-treated MMT, because solvent (acetic acid) can act as a carrier to transport MA into hydrophilic silicate.[6] MA has a flat molecular structure in which the greatest length is about 5.126 Å, as depicted in Figure 6. This scheme also reveals that the incorporation of excess MA into acid-treated MMT extends its gallery spacing.

Because ethylene–propylene–diene rubber (EPDM) is a widely used rubber, EPDM/clay composites should have great commercial potential. However, EPDM does not include any polar groups in its backbone; therefore, the homogeneous dispersion of clay layer in an EPDM matrix would be difficult to realize. In this article, authors introduced MA functional groups into MMT galleries to produce MA-intercalated MMT (MAM). EPDM can be blended with MAM to form a ternary molecular structure (MMT-MA-

EPDM) in the presence of benzoyl peroxide (BPO), as depicted in Figure 6. In such a structure, MA serves as a modifying additive for the EPDM matrix and as a swelling agent for MMT. Then the long molecular chains of the EPDM are easy to diffuse into the galleries of MMT and the homogeneous dispersion of clay layer in the EPDM matrix is successfully realized.

However, there is no literature about the preparation of EPDM/MAM. This work is the first report on the fabrication of the EPDM-MMT nanocomposites using MA as a reactive reagent that acts both as a modifying additive for the EPDM matrix and as a swelling agent for the MMT. At the same time, MA also acts as a vulcanizing agent for EPDM matrix and as a bridge to bond MMT with EPDM matrix. The influence of MA on the morphology and mechanical properties of the EPDM/MAM nanocomposites are investigated.

EXPERIMENTAL

Materials

The source MMT with a cation-exchange capacity of 110 meq/100 g was purified and screened by a 325-mesh sieve. EPDM was purchased from Yangzi Petrochemical Co. (Nanjing, China), with ethylene content of 70%, ENB type and ML1 + 4100°C = 70. MA and BPO were supplied by Shanghai Chemical reagent Co. (Shanghai, China) and purified by recrystallization. Other reagents grade chemicals were used without further purification.

Preparation of MA-delaminated MMT

Approximately 50 g of the crude MMT was introduced into 2 L of a 1M HCl solution in a beaker at room temperature. The resulting slurry was magnetically stirred for 8 h. The pH of the slurry was adjusted to 3.0–4.0. The MMT was then separated by filtering and washed thoroughly with distilled water several times until the filtrate had a pH value of 7.0. Following washing, the obtained solid material was dried at 160°C overnight. The final product after grinding was a fine powder with as-received color. The delamination process of MMT was controlled and monitored by X-ray diffraction (XRD). The acid-delaminated MMT was then further treated with MA. A 250-mL flask was charged with 50 g of MA, 50 g of acid-treated MMT, and 100 mL of acetic acid. The slurry was magnetically stirred for 12 h. The resulting slurry was dried in a rotary evaporator at 60°C and subsequently dried in an oven at 70°C for 24 h under vacuum. The final MA-intercalated MMT (MAM) in the form of fine powder was screened by a 325-mesh sieve and kept in a desiccator.

Nanocomposites preparation

EPDM (9 g) and MAM (1 g) were melt-mixed in a HAAKE Rheometer RC90 (Haake Co. Germany) for 5 min at 90°C and at a rotor speed of 136 rpm, and this was followed by the addition of 0.1 g BPO, the mixing lasted for another 5 min. The resultant mixture was pressed into sheets on a two-roll mill at ambient temperature and was compression-molded at 175°C at an optimum cure time to yield a rubber vulcanizate. The resultant nanocomposites are termed EPDM/MAM-5 throughout this article, where 5 is the weight percent of MMT. The nanocomposites composed of 8.5 g EPDM and 1.5 g MAM or 8 g EPDM and 2 g MAM were prepared as widely described, and were termed EPDM/MAM-7.5 and EPDM/MAM-10, respectively. For comparison, maleated EPDM (EPDM-g-MA) was also prepared as widely described.

Characterization

XRD measurements were made directly from MMT and MAM powders. The dispersion of clay in polymer matrix was evaluated with XRD measurements carried out on films. All XRD measurements were performed on a X'TRA XRD (ARL Co., Switzerland) with CuKα radiation (1.54 Å) and the patterns were recorded in the reflection mode for $2\theta = 1°–10°$ at a scanning speed of 2°/min. The basal spacing of the MMT was estimated from the (001) peak in the XRD pattern. The morphology of EPDM/MAM nanocomposites was performed with a JEM-200 CX transmission electron microscope (JEOL Co., Japan) using 200 kV accelerating voltage. Samples were embedded in epoxy resin, cured at 60°C overnight, and subsequently microtomed at room temperature into ultrathin slices (<100 nm thickness), using a Reichert-Jung Ultracut E microtome. Section were collected with 300-mesh copper grids and were observed without any further modification or coating. The morphology of the broken surface of tensile samples was observed on 650× scanning electron microscopy (Hitachi Co., Japan). The operation voltage is 20 kV. All the samples were gold-coated by means of an IB3 (Eiko Engineering Co. LTD., Japan) sputtering apparatus, before observation.

The thermogravimetric analysis was done on TA 2100-SDT 2960 (PerkinElmer Co., United States), with a temperature ramp of 20°C/min under N2 atmosphere from 25 to 800°C. The dynamic mechanical thermal analysis was carried out on a DMTA V (Rheometric Scientific Co., United States) in the tension mode, using rectangular samples. The sample was subjected to a cyclic tensile strain with amplitude of 0.2% at frequency of 10 Hz, and a static force of 0.1N was used. The temperature ramp was 3.0°C/min and the scanning range was from −90 to 50°C.
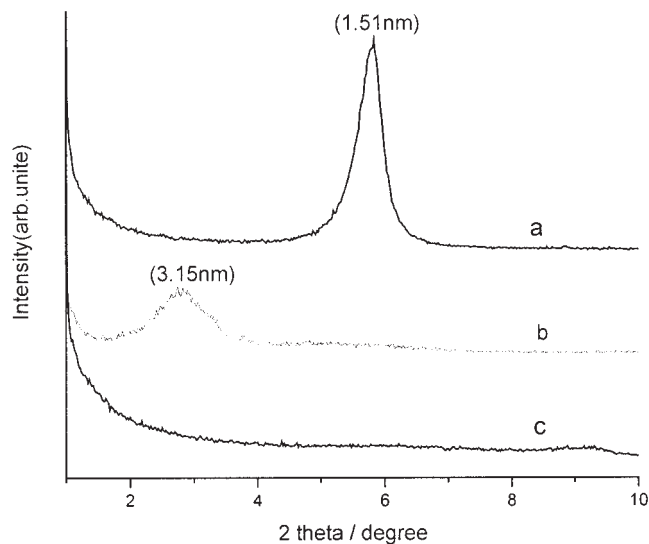
Figure 1 XRD patterns of MMT (a) pristine MMT, (b) acid-delaminated using 1M HCl, followed by drying at 160°C overnight, (c) MA treated MMT (MAM).

The tensile strength, elongation at break, and modulus were measured using an Instron-4200 (Instron Inc., United Kingdom) at a crosshead speed of 500 mm/min, using ASTM D 412 method. The result reflects an average of five specimens and all the mechanical properties were tested at 23°C.

## RESULTS AND DISCUSSION

Structure and morphology

The commonly used layered MMT for the preparation of polymer/layered silicate nanocomposites belongs to the general family of 2 : 1 layered or phyllosilicate. Their crystal structure consists of layers made up of two tetrahedrally coordinated silicon atoms fused to an edge-shared octahedral sheet of either aluminum or magnesium hydroxide. Stacking of the layers lead to a regular van der Waals gap, which provides a large cohesive energy between the layers called the interlayer or gallery. As a consequence of the high layer-to-layer interactions, the intercalation of polymer chains in between the MMT platelets is greatly impeded, being thus a necessary layer surface treatment to facilitate the intercalation and further exfoliation of the clay.

XRD is a useful technique for the characterization of clay and polymer/clay nanocomposites. It allows the precise measurement of silicate layer spacing and monitors the intercalation behavior of surfactants and polymer chains. In this work, an acid treatment route was used to delaminate MMT partially before the incorporation of the MA swelling agent. For monitoring the interlayer space after treatment, the XRD patterns of as-received MMT subjected to HCl and MA

treatments are depicted in Figure 1. The d-spacings of the MMT before and after treatment are calculated using the Bragg's equation, according to the angle of 001 diffraction peak, $2d \sin\theta = \lambda$, where λ corresponds to the wave length of the X-ray radiation used in the diffraction experiment, d is the spacing between diffraction lattice planes, and θ is the measured half diffraction angle or glancing angle).

It can be seen that the characteristic diffraction peak of pristine MMT was at $2\theta = 5.84°$, corresponding to a basal spacing of 1.51 nm. The 2θ d001 of acid-treated MMT is observed at 2.78°, corresponding to a basal spacing of 3.15 nm. This finite expansion of gallery height is associated with proper thermal and acid treatment.[10] To further delaminate the MMT layers, partially delaminated MMT was exposed to a mixed MA and acetic acid solution and stirred for 12 h. XRD traces of MAM (Fig. 1(c)) indicate the absence of diffraction peaks, which clearly reveals that the MMT is further delaminated. The result implies that the gallery spacing of MMT is larger than 3.15 nm. MA can easily enter the galleries of acid-treated MMT, because solvent (acetic acid) can act as a carrier to transport MA into hydrophilic MMT.

As shown in Figure 2, the EPDM/MAM-5 and EPDM/MAM-7.5 have no visible diffraction peaks in the measured angle scope. According to the literature,[8–11] the absence of the characteristic d001 diffraction peak of clay is the strong evidence for the formation of exfoliated or disordered nanocomposites. As far as exfoliated or disordered structure of MMT nanocomposites is concerned, no more diffraction peaks are visible in the XRD patterns either because of too much large spacing between the layers (i.e., exceeding 8 nm in the case of ordered exfoliated structure) or because the nanocomposites do not present ordering anymore. However, a different situation is observed in
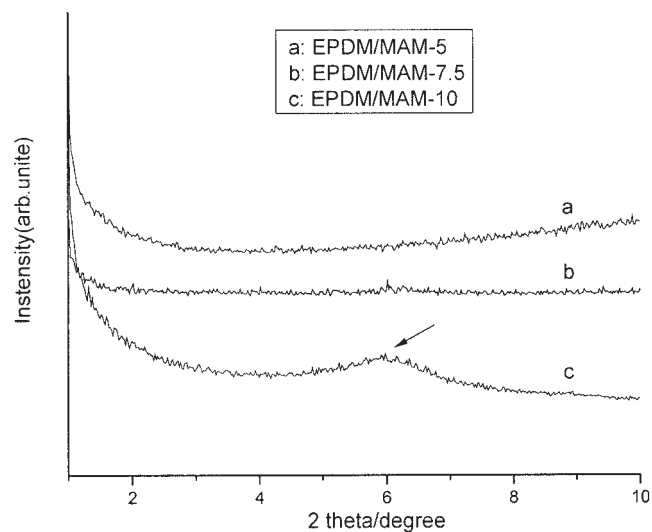
**Figure 2** XRD patterns of EPDM/MAM nanocomposites.
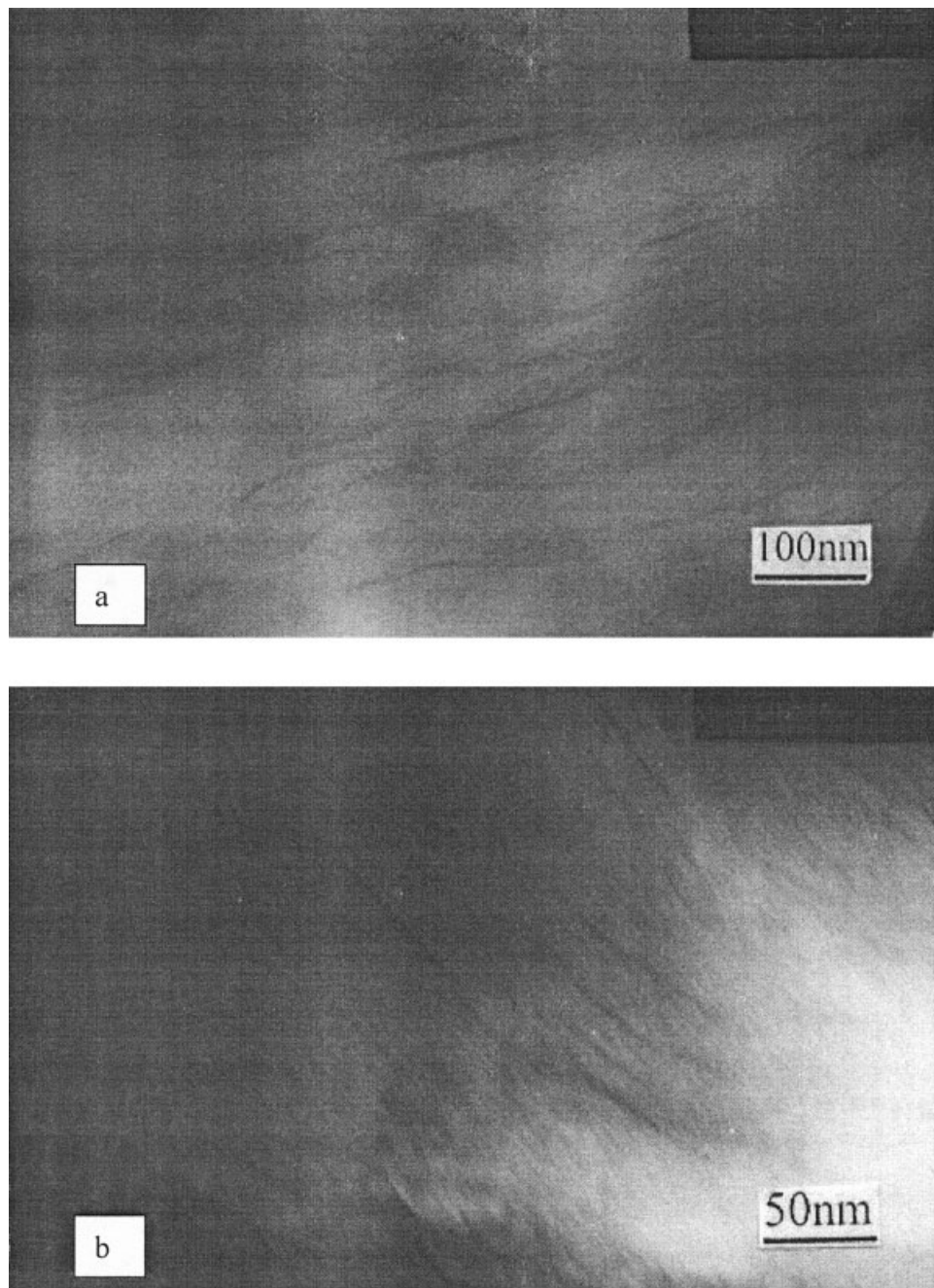
Figure 3 Typical TEM micrographs of EPDM/MAM-7.5 nanocomposite showing (a) formation of exfoliated MMT layers in the nanocomposite and (b) enlarged image of exfoliated MMT layers.

the XRD patterns of EPDM/MAM-10, where a broad peak (black arrow) is visible, and it indicates that some layer structure of the exfoliated MMT rearranged in EPDM/MAM-10 nanocomposite, which was encountered at higher filler content.

It should be noted that in the exfoliated or delaminated state where the periodic arrangement of clay is lost, XRD does not provide definitive information regarding the structure of the nanocomposites. In contrast to the global averaging of XRD, conventional TEM can provide information in real space on mor-

phology and spatial distribution of the various phases. When XRD data exhibit featureless diffraction patterns, it is necessary to use TEM to determine the nature of the hybrids and to provide additional information.
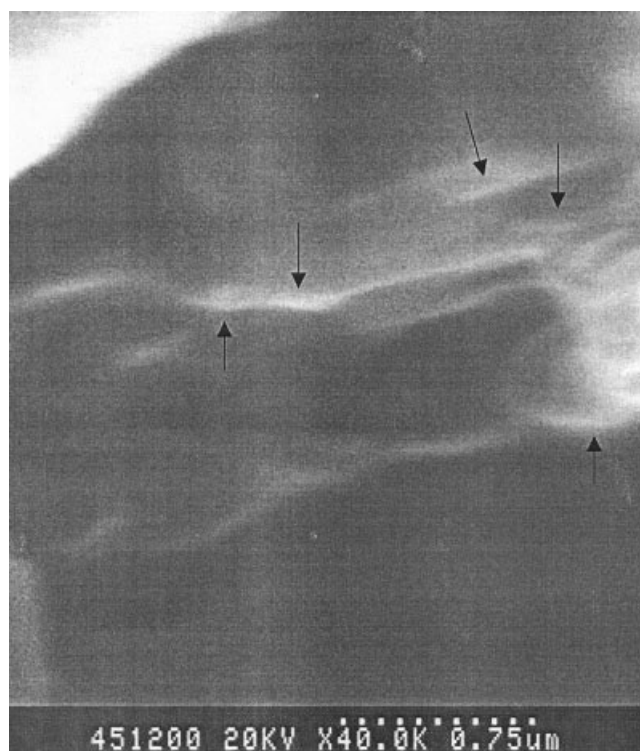
Typical TEM micrographs of EPDM/MAM-7.5 nanocomposite are shown in Figure 3. In the micrographs, the bright field belongs to the EPDM matrix or blank, the dark lines are the transverse sections of silicate platelets. It can be seen that all the MAM are exfoliated and dispersed uniformly in the EPDM ma-
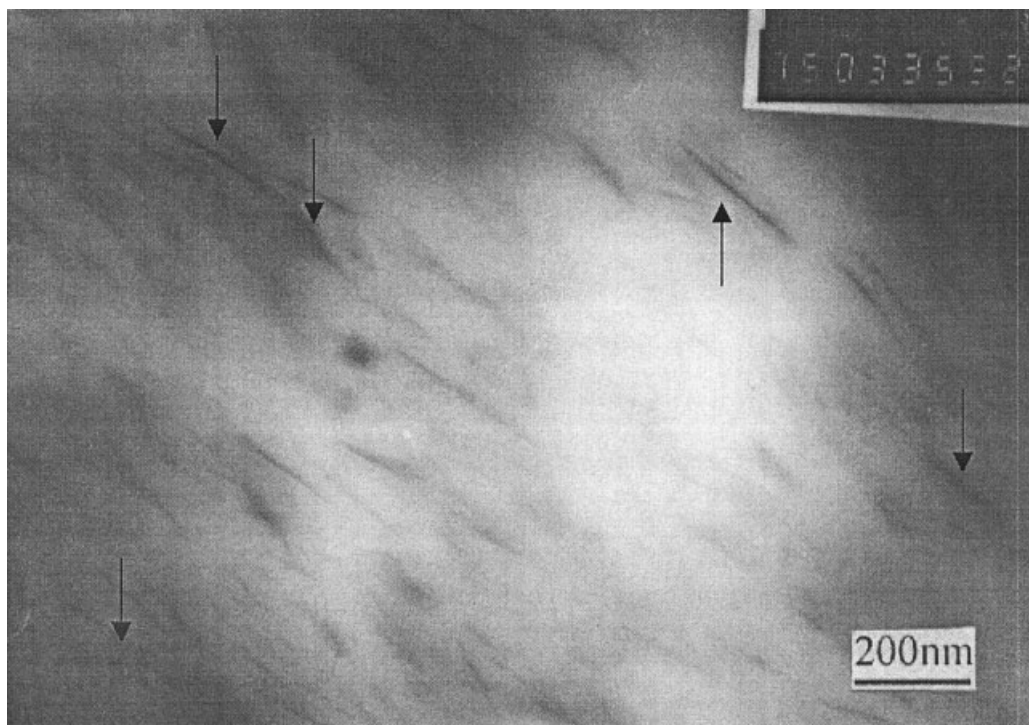
Figure 4 Typical TEM micrographs of EPDM/MAM-10 nanocomposite. Black arrows indicate some layered structure of the exfoliated MMT rearranged in EPDM matrix.

trix, and this result is consistent with the conclusion from XRD. From Figure 3, the MMT layer exhibits a thickness of 1–2 nm and a length of about 200 nm, indicating that the MMT layers have a very large aspect ratio. However, the average thickness of MMT platelets in other nanocomposites[2–5,9] is also somewhat higher than that of a single clay layer, which should be about 1 nm. There are two possible reasons for this discrepancy. One possibility is that the platelets appear to be larger in the image than they actually are, because of inaccurate focusing in TEM. Another possibility is that the microtoming direction is not perfectly perpendicular to the surface of the platelets, and so the image is of a tilted platelet that appears to be thicker than it actually is. Additionally, from Figure 3(b), it is evident that the spacing between the layers is ≥10 nm, which is consistent with XRD. However, a different situation is observed in the TEM micrograph (Fig. 4) of EPDM/MAM-10, where the laminar stacking (Black arrows) of the MMT layers is visible, and it indicates that some layered structure of the exfoliated MMT rearranged in EPDM/MAM-10 nanocomposite, which is consistent with XRD.

Figure 5 shows a typical SEM micrograph of the break surface of tensile samples of EPDM/MAM-7.5 nanocomposite. Exfoliated MMT layers (black arrows) can be readily seen in the SEM micrograph and dispersed uniformly in the EPDM matrix and this result is consistent with the conclusion from XRD and TEM. A micrograph of the sample reveals that the interface

Figure 5 Typical SEM micrograph of EPDM/MAM-7.5 nanocomposite. Black arrows indicate MMT layers.

between the individual MMT layers and EPDM is not clear. This means that the MAM layers could be well-dispersed in EPDM matrix and that the EPDM matrix could contact well with MMT through the formation of a ternary molecular structure (MMT-MA-EPDM) as a result of the presence of MA. In the present work, MA was selected to open the interlayer space of MMT, at the same time, it was adopted to introduce stronger interactions between EPDM and MMT, and then to increase the potential binding energy of the whole system by the introduction of polar groups, such as –COOH, along the gallery of silicate. On the other hand, according to the self-consistent field (SCF) depicted by Singh and Balazs, the enhanced miscibility between the organically modified clay and the polymers with higher number of branches is primarily due to the compactness of the macromolecules.[12] EPDM can be blended with MA to form comb chain in the presence of BPO. The radius of gyration of the polymers decreases as the number of branches increases, and the polymer can more easily interact with and interpenetrate MMT layer.

From the results of XRD, TEM, and SEM, it can be concluded that EPDM could be blended with MAM to form exfoliated EPDM/MAM nanocomposites, which constituted of a ternary molecular structure (MMT-MA-EPDM), in the presence of BPO. In such a structure, MA serves as a modifying additive for the EPDM matrix and as a swelling agent for MMT. Then the long molecular chains of the EPDM are easy to diffuse into the galleries of MMT and the homogeneous dispersion of MMT layer in the EPDM matrix is successfully realized. Conceptual figure of forming process of exfoliated EPDM/MAM nanocomposites is depicted in Figure 6. In such a compatible structure, grafted MA acts as a vulcanizing agent for EPDM matrix and as a center or a bridge to bond MMT with EPDM together. To further confirm the excellent properties of exfoliated EPDM/MAM nanocomposites constituted of a ternary molecular structure (MMT-MA-EPDM), the thermal and mechanical properties of nanocomposites was investigated and discussed as follows.

Thermal properties

The introduction of silicate can improve the thermal properties of the polymer matrix was reported by many other researchers.[13] The TGA analysis of EPDM/MMT nanocomposites is shown in Figure 7. It can be seen that the EPDM/MMT nanocomposites display higher thermal resistance than that of EPDM-g-MA because of the presence of clay. Resistance to thermal degradation is improved when the MMT content is increased up to 7.5 wt %. The increase in thermal resistance resulted for the fact that nanosized MMT layers, 1–2 nm thick and about 200 nm long, are able to sustain high temperature and to retard the heat
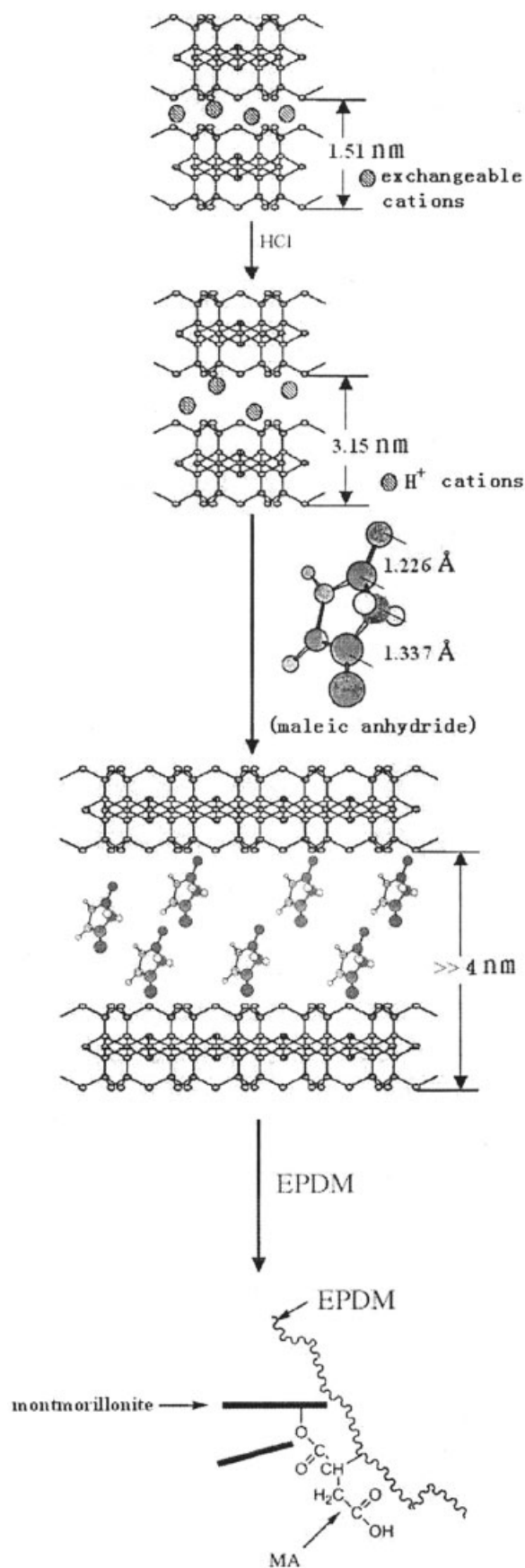
diffusion into EPDM matrix. With further increase in MMT content, no further increases in thermal resistance of the composites were observed. One possibility is that with high MMT content, for example 10%, MMT coagulated in the EPDM matrix and could not disperse very well, and this result is consistent with the conclusions from XRD and TEM. Another is that the acid-pretreated MMT contains unreacted MA when MMT content is ≥10 wt %.

The dynamic mechanical thermal analysis is a good method to examine the degree of filler-matrix interaction, and the change in glass transition temperature (Tg) of the polymer/clay nanocomposites. Figure 8 shows the effect of MAM on storage modulus of the nanocomposites. It is evident from Figure 8 that the storage modulus of EPDM/MAM is large than that of EPDM-g-MA as a function of temperature, because of the greater reinforcing effect of the MAM. For example, the storage modulus at 25°C of the EPDM/MAM-7.5 is 3.9 times higher than that of the EPDM-g-MA. This beneficial effect is believed to arise from an improvement of the compatibility between the MMT and EPDM matrix associated with MA addition. Consequently, a ternary molecular structure of MMT-MA-EPDM with MA as a center in the grafted EPDM can develop in these nanocomposites (Fig. 6). Moreover, the ternary structure can promote the nano-scale dispersion of MMT within EPDM matrix, then storage modulus increase significantly upon formation of the nanocomposites. The increase in storage modulus is most manifest in the case of the EPDM/MAM-7.5, and this is consistent with the conclusion above.
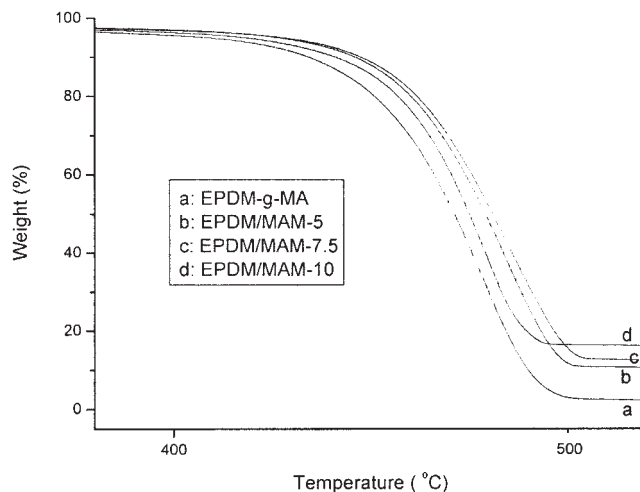
On the other hand, it can be seen that the Tg increased slightly with the amount of MMT (Table I). The enhancement in Tg is most manifest in the case of the EPDM/MAM-10 nanocomposite, which enhanced from −35.0 to −29.9°C. This slight shift to higher temperature is because the mobility of EPDM molecular chains is restricted by the presence of MMT layers.

Mechanical properties

Generally, mechanical properties of a polymer filled with inorganic clay are related to the nano-scale thickness of the interlayers and the degree of interfacial interactions. In conventional nanocomposites, however, the interfacial bonding between the matrix and the reinforcing materials is relatively poor. Thus, MA is used to improve the interfacial adhesion between them. On the other hand, the MA functional group of EPDM/MAM nanocomposites tends to exfoliate the galleries of MMT, leading to nano-scale dispersion of reinforcement within the polymer matrix. The uniform dispersal of the MAM nano-layers in the EPDM matrix is considered to form a physical barrier against a growing crack, which leads to an increase in the

Figure 7 TGA curves of EPDM/MMT nanocomposites with different content.

resistance to tearing. These observations indicate that the exfoliation of MMT in the EPDM matrix can offer the nanocomposites effective enhancement in toughness and strength as well as stiffness.

Table I shows that exfoliation of MMT in the EPDM matrix provided EPDM/MAM nanocomposites with outstanding mechanical properties. It can be seen that relative to the EPDM-g-MA, all of the nanocomposite show high enhancement in tensile, tear, and modulus properties. Compared with the EPDM-g-MA, the nanocomposite from EPDM/MAM-7.5 shows the highest tensile strength, enhanced by about 94.5%, which is because of the nano-scale dispersion of MA-modified MMT within the EPMD matrix. With further increase in clay content, the tensile strength and the

Figure 6 Conceptual figure of forming process of exfoliated EPDM/MAM nanocomposites.
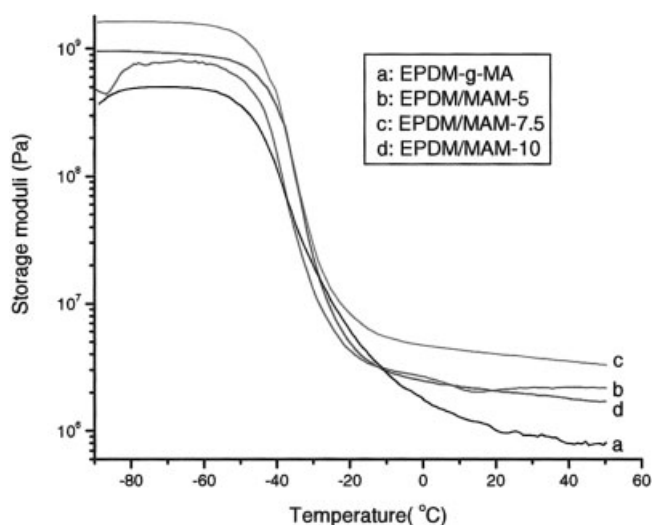
Figure 8 Storage modulus of EPDM and EPDM/MAM nanocomposites. [Color figure can be viewed in the online issue, which is available at www.interscience.wiley.com.]

TABLE I
Mechanical Properties of the EPDM/MAM Nanocomposites

	MMT content (%)	Stretch strength (MPa)	Elongation at auto break (%)	Young's modulus (MPa)	Storage modulus at 25°C (10^6 Pa)[a]	T_g (°C)[a]
EPDM-g-MA	0	2.905	2165.3	1.851	1.0	−35.0
EPDM/MAM-5	5	4.492	2493.0	2.021	2.1	−32.2
EPDM/MAM-7.5	7.5	5.651	2237.7	2.266	3.9	−31.2
EPDM/MAM-10	10	4.712	2175.0	2.367	2.0	−29.9

[a] Determined by dynamic mechanical thermal analysis (DMTA).

elongation-at-autobreak of the nanocomposites decreased, but the Young's modulus increased slightly. From Figure 4, we can see some clay aggregates formed by the high clay content. The formation of large silicate stacks, which effectively reduces the interfacial area available for polymer/clay interaction and acts as stress concentrators, results in poor mechanical properties.

CONCLUSIONS

In this article, EPDM/MMT nanocomposites were successfully prepared by MA-modified MMT and EPDM to form a ternary molecular structure (MMT-MA-EPDM) in the presence of BPO. MA acts both as the intercalation agent for MMT and as a vulcanizing agent for EPDM matrix. It also acts as a compatibilizer for the EPDM and MMT phases. The XRD patterns and the TEM photographs show that MMT particle are exfoliated into nanoscaled layers, which are dispersed throughout EPDM matrix. From DMTA results, it can be seen that a strong rubber-filler interaction in the nanocomposites is manifested in the measured temperature scope and MMT addition increases the Tg of nanocomposites. There is some enhancement in degradation behavior between the nanocomposites and EPDM-g-MA. Additionally, the nanocomposites exhibit great improvement in tensile strength and modulus, as well as elongation-at-break. However, those mechanical properties and resistance to thermal degradation of the nanocomposites begin to decrease with the continuously increasing amount of MMT.

References

1. Okada, A.; Kawasumi, M.; Usuki, A.; Kojima, Y.; Kurauchi, T.; Kamaigoto, O. Polym Prepr (Am Chem Soc Div Polym Chem) 1987, 28, 447.
2. Usuki, A.; Tukigase, A.; Kato M. Polymer 2002, 43, 2185.
3. Zheng, H.; Zhang, Y.; Peng, Z. L.; Zhang, Y. X. J Appl Polym Sci 2004, 92, 638.
4. Sinhan Ray, S.; Yamada, K.; Okamoto, M.; Ogami, A.; Ueda, K. Chem Mater 2003, 15, 1456.
5. Zanetti, M.; Costa, L. Polymer 2004, 45, 4367.
6. Tjong, S. C.; Meng, Y. Z.; Hay, A. S. Chem Mater 2002, 14, 44.
7. Giannelis, E. P. Adv Mater 1996, 8, 29.
8. Carrado, K.; Xu, L. Chem Mater 1988, 10, 1440.
9. Han, B.; Ji, G. D.; Wu, S. S.; Shen, J. Eur Polym J 2003, 39, 1641.
10. Tjong, S. C.; Meng, Y. Z.; Xu, Y. J Appl Polym Sci 2002, 86, 2330.
11. Du, X. S.; Xiao, M.; Meng, Y. Z.; Hung, T. F.; Rajulu, A. V.; Tjong, S. C. Eur Polym J 2003, 39, 1735.
12. Singh, C.; Balazs, A. C. Polym Int 2000, 49, 469.
13. Vaia, R. A.; Giannelis, E. P. Macromolecules 1997, 30, 7990.